NICE du 16 au 20 MAI 1983

Influence of Noise and Quantization Error in Microwave
Holography on Holograms and Image Reconstructions

P.Ballerscheff and F. Arndt

Microwave Department University of Bremen,
Kufsteiner Str., NW 1, D-2800 Bremen 33,
W.-Germany

RESUME

L'holographie des micro-ondes est une méthode complexe
dans la technique radar servant à identifier la forme
d'objets métalliques plans et tridimensionaux. La
simulation numérique de deuxième ordre (transformation
discrète de Fresnel- Kirchhoff) des hologrammes offre
l'avantage de pouvoir étudier l'extension appropriée
des hologrammes et l'influence de l'analyse discrète
afin d'améliorer la précision de la méthode
de représentation. L'usage de l'algorithme "Fast Fourier
Transform" assure une reconstruction numérique rapide des
images avec laquelle une identification sûre des objets
est possible. Pour les signaux au bruit les problèmes ne
sont pas encore complètement résolus. Cette publication
recherche systématiquement l'influence des erreurs de
bruit et de quantification (pour amplitude et phase) sur
les hologrammes et la reconstruction des images. On
démontre qu'avec une superposition numérique appropriée
des hologrammes une identification d'objets rectangu-
laires et circulaires est possible même lorsque le
rapport signal-bruit est d'environ 1/5. La publication
démontre de plus qu'une définition appropriée d'un
critère d'acuité pour l'identification d'objets amène
à la détermination de la distance sans aucune ambiguïté.
Cette détermination peut être réalisée par des procédés
traditionnels d'optimisation numérique.

SUMMARY

Microwave holography is a versatile tool in radar to
identify the shape of planar as well as of three-dimen-
sional metallic objects. Numerical second-order simu-
lation (discrete Fresnel-Kirchhoff-Transformation) of
holograms yields the advantage that the suitable expan-
sion of the holograms and the sampling influence can be
systematically investigated in order to improve the accu-
racy for the imaging method. The use of the Fast Fourier
Transform algorithm provides quick computer recon-
struction of the images where clear identification of the
objects is possible. For noisy signals the problems are
not yet completely solved. The paper investigates sys-
tematically the influence of noise and quantization
error (for amplitude and phase) on holograms and image
reconstruction. It is shown that by suitable computer
superposition of holograms an identification of rectan-
gular and circular objects is possible even if the sig-
nal-to-noise ratio is about 1/5. The paper shows further
that a suitable definition of a clearness criterion for
the identification of objects leads to an unambiguous
range determination which can be carried out by common
numerical optimization procedures.

Influence of Noise and Quantization Error in Microwave
Holography on Holograms and Image Reconstructions

1. INTRODUCTION

Microwave holography[1-6] is a useful technique for imaging
remote or inaccessible metallic objects. As has already
been shown, a clear identification of two- and three-
dimensional objects is possible, if the necessary con-
ditions for sampling theorem, hologram plane dimension
and window functions are held[1,3,6].

Although for hologram formation in reality scattered
field intensity and phase of an illuminated object are
measured, it has turned out to be advantageous[1,3,6] to
investigate the necessary hologram formation conditions
by numerical computer simulation using the FRESNEL-
KIRCHHOFF's diffraction integral. Further, the computer
simulation of holograms, taken from two-dimensional as
well as from three-dimensional objects, has been proved
to be an appropriate tool to perform complicated experi-
ments, where practical measurements are too expensive or
in fact impossible. The image reconstruction step is
carried out digitally, where the FRESNEL-approximation
enables the use of standard signal processing techniques
like the Fast-Fourier-Transform (FFT).

Systematic errors at the hologram formation (like loss of
information by underscanning or by band limitation in the
hologram plane) have already been extensively investi-
gated[1,3,6]. By suitable choice of the hologram formation
parameters those errors can largely be eliminated.

Stochastic disturbance of the hologram formation however,
like noise caused by incomplete reflection characteristic
of the illuminated object and by spurious noise sources
in space, or quantization error caused e.g. by the in-
sufficiency of the measuring equipment, have not yet been
investigated systematically. This paper is a contri-
bution to remove this lack.

It will be shown, that suitable superposition of noisy
complex hologram function values leads to a clear iden-
tification of the reconstructed image even if the sig-
nal-to-noise ratio is much more less than 1. The depen-
dence of the amplitude and phase quantization error on
the information contents in holograms is systematically
investigated at the examples of a circular and quadratic
metallic plate.

The paper investigates furthermore suitable criterions
for numerical range determination, which can be carried
out by common and wellknown optimization procedures. An
appropriate clearness criterion leads to additional in-
formation which allows to locate the range up to an
error of about 1% even if the hologram function is noisy.
By analysing the real and imaginary part of the recon-
structed image function it is possible to separate mutu-
ally distant parts of three-dimensional objects, which is
demonstrated at the example of two quadratic metal
plates of different sizes mounted in different distances.

2. THEORY

The computer simulation of the diffracted wave at the
point P_0 (x_0, y_0) in the hologram plane (Fig. 1) is based
on the FRESNEL-KIRCHHOFF's diffraction integral, which is
written in its discrete form[6], where the z-dimension of
the object (Fig. 1b) is subdivided into P planes with the
dimensions $\Delta x_p \cdot M$, and $\Delta y_p \cdot N$ and the complex hologram
function $\underline{U}_{il}$ is taken for $I \cdot L$ points with the sample distance
$\Delta x_0, \Delta y_0$:

$$\underline{U}_{il} = j \frac{1}{2\lambda} \sum_{p=1}^{P} \Delta x_p \Delta y_p \Delta z_p \sum_{m=0}^{M-1} \sum_{n=0}^{N-1} 0_{mnp} C_s \frac{e^{-jks_{mnp}}}{s_{mnp}}$$

$$\frac{e^{-jkr_{mnilp}}}{r_{mnilp}} \left\{ \cos(\vec{v}_{mnp}, \vec{r}_{mnilp}) - \cos(\vec{v}_{mnp}, \vec{s}_{mnp}) \right\} \quad (1)$$

with

λ = wavelength

$k = 2\pi/\lambda$

$0_{mnp} \cdot C_s$ = field distribution of the
diffracting interface (ob-
ject planes)

$s_{mnp} = \left\{ (x_{os} - x_q - \Delta x_p m)^2 + (y_{os} - y_q - \Delta y_p n)^2 + z_p^2 \right\}^{1/2}$

$r_{mnilp} = \left\{ (\Delta x_0 i - x_q - \Delta x_p m)^2 + (\Delta y_0 l - y_q - \Delta y_p n)^2 + z_p^2 \right\}^{1/2}$

$\vec{v} = \vec{n} \, v$

$$v = z \left\{ 1 + (\frac{\partial z}{\partial x})^2 + (\frac{\partial z}{\partial y})^2 \right\}^{1/2}$$

$$\cos(\vec{n}, \vec{r}) = \frac{r^2 + v^2 - D_1^2}{2 \, rv} \quad ; \quad \cos(\vec{n}, \vec{s}) = -\frac{s^2 + v^2 - D_2^2}{2 \, sv}$$

$$D_1^2 = (x_0 - x - \frac{\partial z}{\partial x} z)^2 + (y_0 - y - \frac{\partial z}{\partial y} z)^2$$

$$D_2^2 = (x_{os} - x - \frac{\partial z}{\partial x} z)^2 + (y_{os} - y - \frac{\partial z}{\partial y} z)^2$$

$\vec{n}$ = direction of the area dF.

The computer image reconstruction is carried out with
the FRESNEL-integral[6] which is described as two-dimen-
sional discrete FOURIER transform of the function
$\underline{G}_{il} = \underline{U}_{il} \cdot \exp \left\{ j \frac{\pi}{\lambda z} \left[(\Delta x_0 \cdot i)^2 + (\Delta y_0 \cdot l)^2 \right] \right\}$:

$$\underline{B}_{mn} = -j \frac{\Delta x_0 \Delta y_0}{\lambda z} e^{jkz} e^{j\frac{k}{2z}\{(x_q + \Delta xm)^2 + (y_q + \Delta yn)^2\}}$$

$$\sum_{i=0}^{I-1} \sum_{l=0}^{L-1} \underline{G}_{il} \, e^{-j\frac{2\pi}{\lambda z}\{(x_q + \Delta xm)\Delta x_0 i + (y_q + \Delta yn)\Delta y_0 l\}} \quad (2)$$
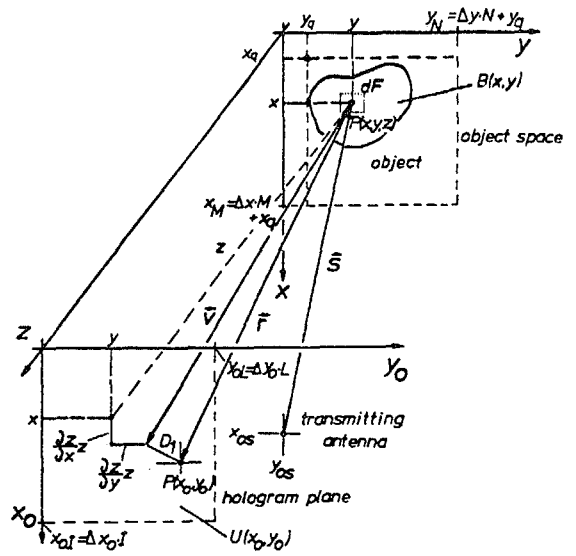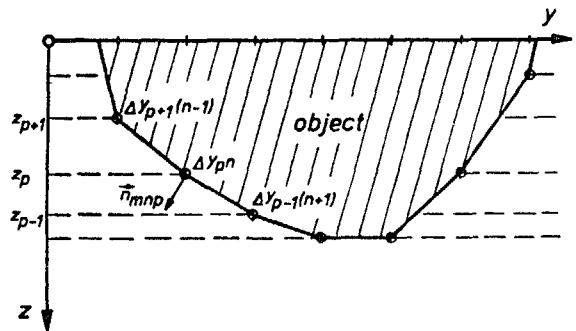

Fig. 1a

Fig. 1b

Fig. 1   Object and hologram plane
a arrangement and related coordinates
b subdivision of the three-dimensional
object space into P planes perpendicular
to the z-coordinate

For the computer simulation of the hologram a window
function

$$WF = rect \left\{ \frac{x_{ov} - x_{oI}/2}{2x_{ope}} , \frac{y_{ov} - y_{oL}/2}{2y_{ope}} \right\} \quad (3)$$

is introduced (Fig. 2a) which suppresses the periodicity
of the hologram function. So e.g. falsifying contri-
butions of inclined object parts (Fig. 2b) are eliminated.
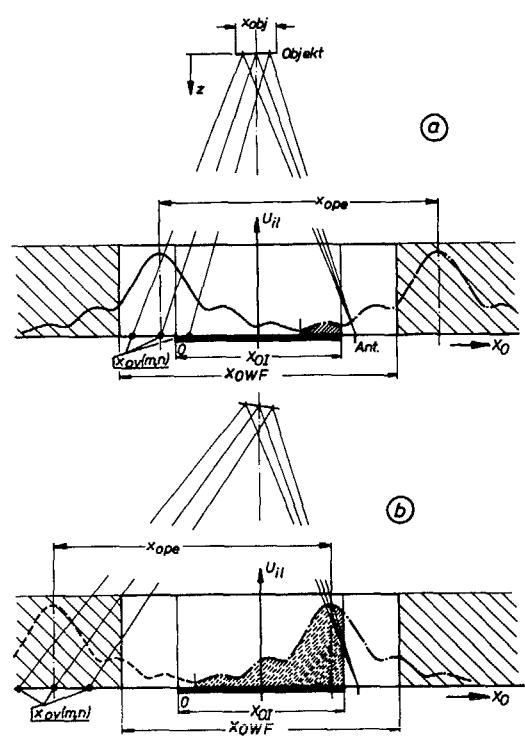
Fig. 2   Window function
           a object parallel to the hologram plane
           b inclined object

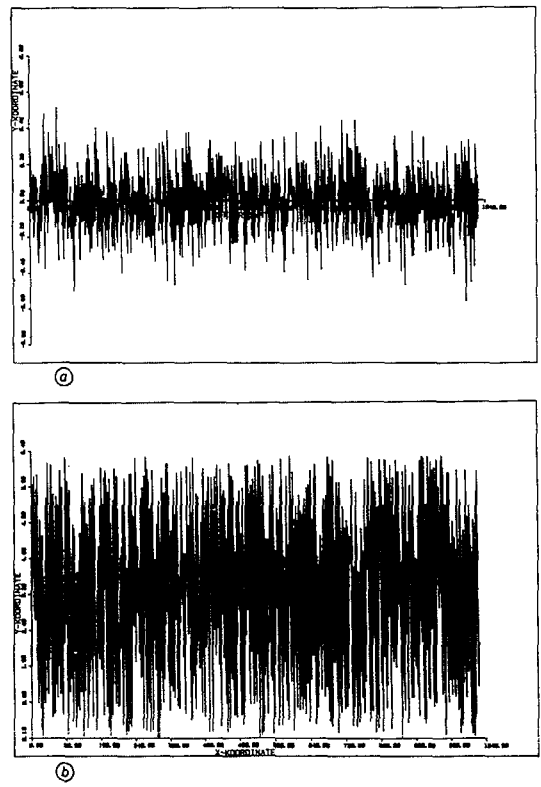Fig. 3   Sequence of 1024 random variables
           a Gaussian distribution for noise amplitude
             simulation
           b uniform distribution for noise phase
             simulation

3. NOISE INFLUENCE

Imperfect back-scattering of the illuminated object leads
to a superposition of a complex noise component $A \cdot \underline{\xi}_{mnp}$ to
the object function $\underline{B}_{mnp} = (O_{mnp} \cdot C_s / s_{mnp}) \cdot \exp(-jks_{mnp})$ in
equation (1)

$$\underline{B}'_{mnp} = \underline{B}_{mnp} + A \cdot \underline{\xi}_{mnp} . \qquad (4)$$

Jamming by noise sources in the measuring space is ex-
pressed by an additional complex noise component $C \cdot \underline{\zeta}$ to
the hologram function $\underline{U}_{il}$ in equation (1)

$$\underline{U}'_{il} = \underline{U}_{il} + C \cdot \underline{\zeta}_{il} \quad , \qquad (5)$$

where A, C are amplitude factors, and $\underline{\xi}, \underline{\zeta}$ complex random
variables which may be functions of location and time. The
statistical parameters, amplitude density p, variance σ^2,
and expected value E, for magnitude (m) and phase (ph) of
the random variables $\underline{\xi}$ and $\underline{\zeta}$ are

$$p(m) = \frac{1}{\sqrt{2\pi}\sigma} e^{-\frac{(\xi,\zeta)^2}{2\sigma^2}} \quad ; \quad \sigma^2 = 1/36 \quad ; \quad E(m) = 0 \qquad (6)$$

$$p(ph) = \begin{cases} 1/2\pi & \text{for } 0 \le \text{arc}(\underline{\xi},\underline{\zeta}) \le 2\pi \\ 0 & \text{else} \end{cases} \quad ; \quad \sigma^2 = \pi^2/3 \quad ; \quad E(ph) = \pi \qquad (7)$$

$\underline{\xi}$ and $\underline{\zeta}$ are simulated numerically. For generation of the
uniformly distributed random phase the $(0,1)$-algorithm[7]

$$z_{j+1} = \frac{a \cdot z_j \, (\text{mod } q)}{q} \qquad (8)$$

is used, where $(a, z_j, q) \in N$; $j = 0, 1, 2, \ldots$; $q = 2^{15}, a \approx 2^8 + 3$
(for 16 bit computer), z_0 is arbitrary but odd. The nor-
mal distribution of the random amplitude is generated by
the uniformly distributed z_k of equation (8)

$$x_j = \bar{x} + \sigma_z \left[\sum_{k=1}^{12} z_k - 6 \right] \qquad (9)$$

where $\bar{x} = 0$ and $\sigma_z = 1/6$. Fig. 3a shows a sequence of
32×32 normal distributed random variables for noise
amplitude simulation, Fig. 3b a sequence of 32×32 uni-
formly distributed random variables for noise phase
simulation.

The influence of noise in the object function $\underline{B}'$ (equa-
tion (4)) on the hologram function $\underline{U}$ and on the image
reconstruction is largely reduced by the transformation
process involved in equations (1) and (2), respectively,
which leads to an averaging of the perturbances. This
effect is demonstrated in Figs. 4, where an arrangement
of a circular disk and a quadratic plate, with a
distance of 2m from each other, is considered as an ob-
ject example (Fig. 4a). Magnitude and phase of the com-
plex object functions are assumed to be disturbed with
a signal-to-noise ratio of about $S/N = 0.5$ (Figs. 4b).
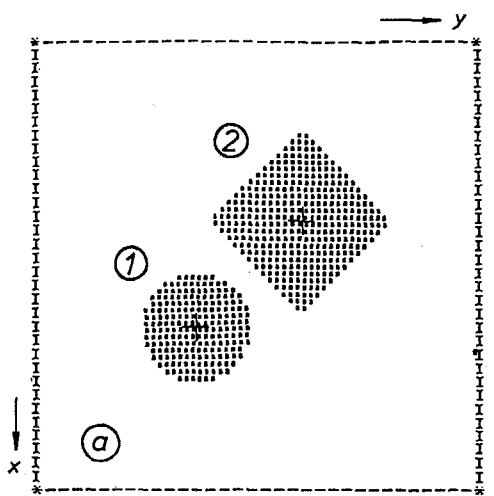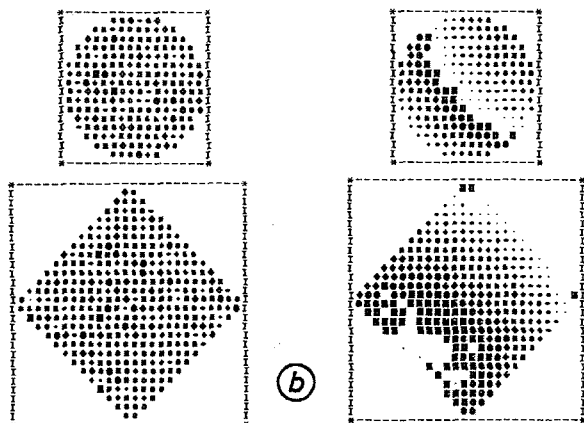

Fig. 4   Reduction of the influence of object noise by
           the diffraction and imaging transformation
           process
           a plane objects: distant from each other by 2m:
             1 circular disk, diameter d=0.5m, center-
             point coordinates $x_1 = 1.25m, y_1 = 0.75m$,
             distance to hologram plane $z_1 = 4m$; 2 quadra-
             tic plate, length of side a=0.62m, $x_2 = 0.8m$,
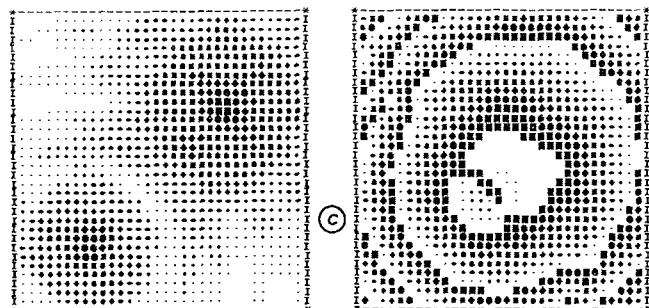 $y_2 = 1.2m$, $z_2 = 6m$

Influence of Noise and Quantization Error in Microwave
Holography on Holograms and Image Reconstructions

The complex hologram function (Fig. 4d) of the disturbed
objects differs only slightly from that one of the un-
disturbed objects (Fig. 4c). Further, the reconstructed
images (Fig. 4e) of the disturbed objects are clearly
identifiable in spite of the original signal-to-noise
ratio S/N=0.5. The above results are numerically con-
firmed by a separate hologram formation of the noise
component ξ_{mnp} in equation (4) alone for the disk as ob-
ject example. The maximum magnitude in the noisy hologram
(Fig. 4h) is only about 1/13 of that one of the undis-
turbed case (Fig. 4g) in spite of an assumed signal-to-
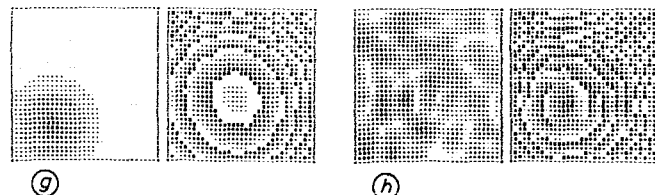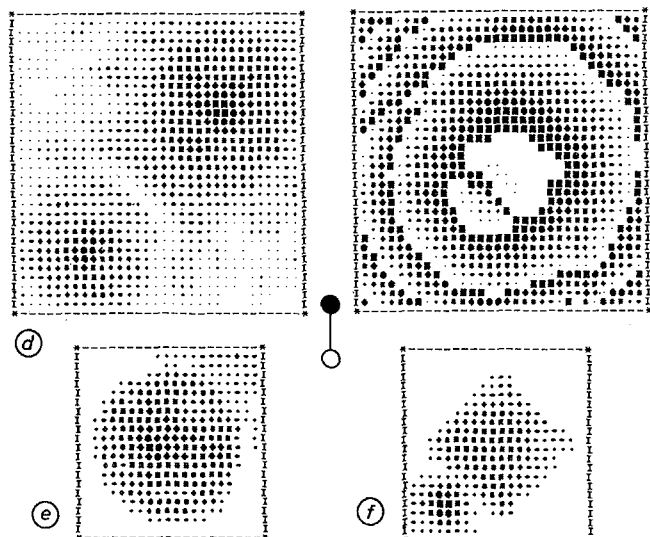noise ratio S/N=0.5 as before.

d   magnitude and phase of the complex hologram
    function of the object arrangement (Fig.4a)
    disturbed according to Fig.4b
e   image reconstruction of the object 1 from
    the hologram formation d
    $x_M=y_N=0.625m$, $M=N=20$, $x_q=0.937m$, $y_q=0.437m$
    $x_{os}=y_{os}=1m$, $\lambda=0.03m$, $z_1=4m$
f   image reconstruction of the object 2 from
    the hologram formation d
    $x_M=y_N=1.016m$, $M=N=20$
    $x_q=0.292m$, $y_q=0.692m$
    $x_{os}=y_{os}=1m$; $\lambda=0.03m$, $z_2=6m$

g

h

g   magnitude of the complex hologram function
    of the undisturbed object 1 alone. Maximum
    absolute magnitude $|\underline{U}|_{max}=0.974$
h   magnitude of the complex hologram function
    of the object noise of object 1 alone.
    Maximum absolute magnitude $|\underline{U}|_{max}=0.074$

b

b   disturbed magnitude and phase of the com-
    plex object function, signal-to-noise ratio
    S/N=0.5

The influence of noise in the hologram function U'
(equation (5)) on the image reconstruction B is averaged
analogously to the object function noise by the corres-
ponding transformation in equation (2).This is demon-
strated in Figs.5a,b. Although the signal-to-noise ratio
of the noisy hologram (Fig. 5a) is S/N=1, the objects 1
and 2 (cf. Fig. 4a) still can be identified (Figs.5b).
For numerical example, again a separate transformation of
noise alone is investigated. Fig. 5e schows the complex
hologram noise component $\underline{\zeta}_{11}$ in equation (5) alone to-
gether with the corresponding image reconstruction (Fig.
5f). The maximum magnitude in the noise image reconstruc-
tion (Fig. 5f) is about 1/3 of that one of the recon-
struction (Fig. 5d) taken from the undisturbed hologram
(Fig. 5c), in spite of S/N=1. Because of the low ampli-
tude density in Fig.5c, however, the noise influence for
this example is more severe than for example Fig. 4h
(1/3 instead of only 1/13).

c

c   magnitude and phase of the complex hologram
    function of the undisturbed object arrange-
    ment of Fig.4a
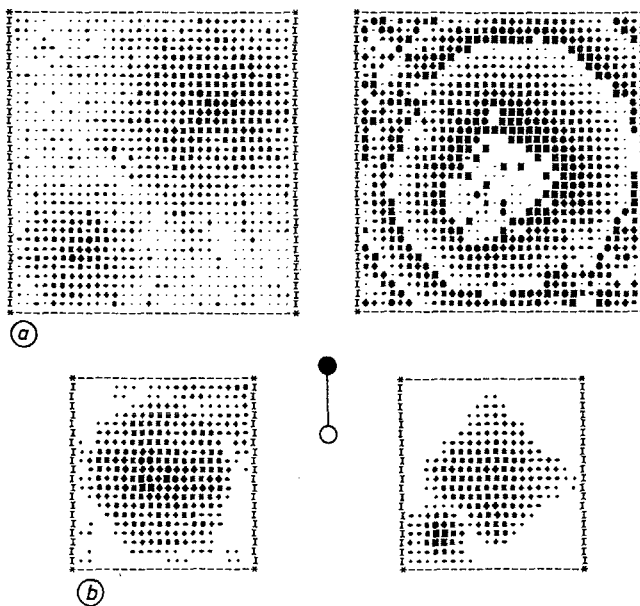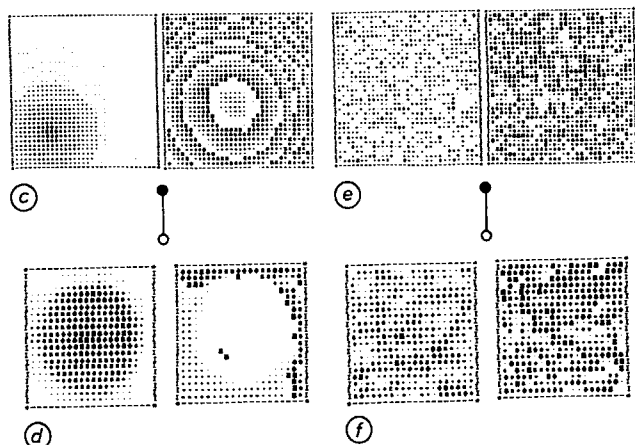

a

b

d

e

f

Fig. 5   Reduction of the influence of hologram noise by
         the imaging transformation process

         a magnitude and phase of the noisy hologram
           according to the object arrangement Fig. 4a
           S/N=1
         b image reconstruction of objects 1 and 2 from
           the noisy hologram a
           (reconstruction data cf. Figs. 4e,f)

Influence of Noise and Quantization Error in Microwave
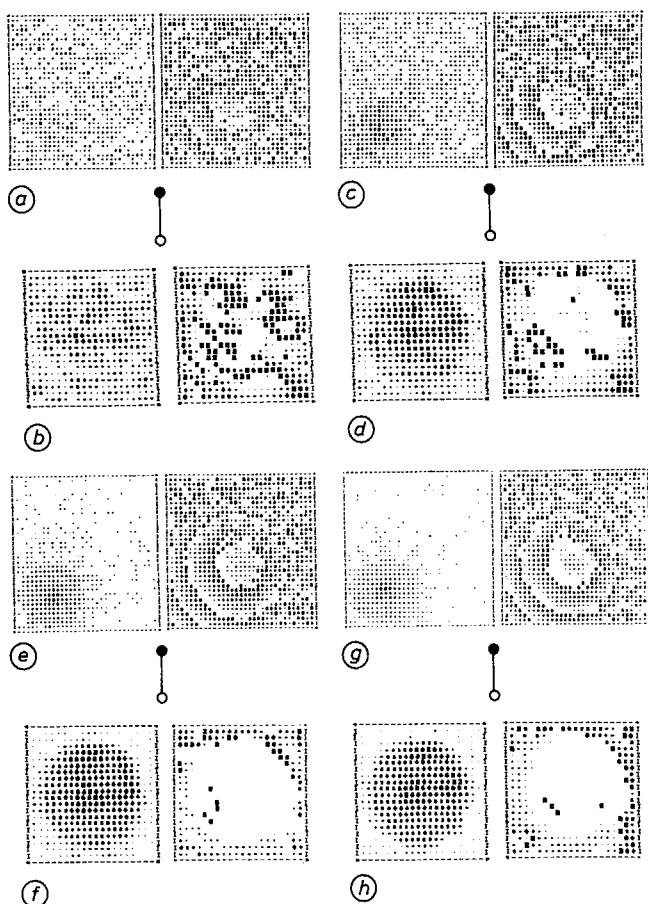Holography on Holograms and Image Reconstructions

Fig.6   Multiple hologram formation and superposition to
        reconstructed images for low information signals
        within heavy noise

        a noisy complex hologram function for object 1
          (cf. Fig. 4a) S/N=1/5
        b image reconstruction from a
        c like a, but 10 superpositions
        d image reconstruction from c
        e like a, but 50 superpositions
        f image reconstruction from e
        g like a, but 512 superpositions
        h image reconstruction from g

c phase and magnitude of the undisturbed hologram
  to object 1 (Fig. 4a) alone $|\underline{U}|_{max}=1$
d image reconstruction from c
  $|\underline{B}|_{max}=5.146$
e phase and magnitude of the hologram noise alone
  $C \cdot |\underline{\epsilon}|_{max}=0.558$
f image reconstruction from e
  $|\underline{B}|_{max}=1.609$

4. QUANTIZATION ERROR

The influence of magnitude and phase quantization in the
hologram function, equation (1), on image reconstruction
is investigated by introducing $\underline{U}_{il}$ in equation (2),

$$\underline{U}'_{il} = (U_{il}+\Delta U_{il})e^{j(\varphi_{il}+\Delta\varphi_{il})} \quad (10)$$

where ΔU_{il} = error of magnitude quantization,

             $\Delta\varphi_{il}$ = error of phase quantization.

The uniform distributed quantization errors in magnitude
(ΔU) and phase ($\Delta\varphi$) show the following properties

$$p(\Delta U, \Delta\varphi)=\begin{cases} 1/\Delta s \text{ for } -\frac{\Delta s}{2} < \Delta U < \frac{\Delta s}{2} \\ 0 \text{ else} \end{cases}, E|\Delta U, \Delta\varphi|=0, \ E|\Delta U^2, \Delta\varphi^2|=\frac{\Delta s^2}{12} \quad (11)$$

Because of the stochastic character of the quantization
errors, like in chapter 3, their influence on image re-
construction is also reduced by the transformation pro-
cess involved. This effect is shown in Fig. 7, where for
better perception the complex hologram function is ex-
hibited perspectively. For 10 quantization steps in
magnitude, and 8 in phase (Fig. 7a), the objects can
still be identified clearly. The limit of identification
is reached for 5 quantization steps in magnitude and 4
in phase (Figs. 7c,d). Because of the lower hologram
function portion of object 1 in the hologram of the two
objects (cf. e.g. Fig. 4g with Fig. 4c) the reconstruc-
ted image of object 1 is more disturbed than that of ob-
ject 2.

In order to eliminate the mutual influence of the two
objects, in Fig. 8 only object 1 (Fig.4a) is investi-
gated. For 5 quantization steps in magnitude and 4 in
phase (Fig. 8) the object 1 (in comparison to Fig.7d)
can still be identified clearly.

If time or location dependency of hologram noise $\underline{\epsilon}$ is
considered, a useful practical application for signal
detection at very poor signal-to-noise ratio levels
(S/N<1) is possible: By multiple hologram formation and
superposition of the results a low information signal
within heavy noise can be reconstructed. This is demon-
strated in Fig. 6. Fig. 6a shows the noisy complex holo-
gram function for object example 1 (cf. Fig. 4a) if the
signal-to-noise ratio is S/N=1/5. As expected a distinct
image in the reconstruction from this noisy hologram can
not be identified (Fig. 6b). For only ten hologram super-
positions (Fig. 6c), however, the object is already re-
cognizable. For 50 and 512 superpositions (Figs.6e,g),
the object can clearly be identified (Figs.6f,h), al-
though the signal-to-noise ratio of the single noisy
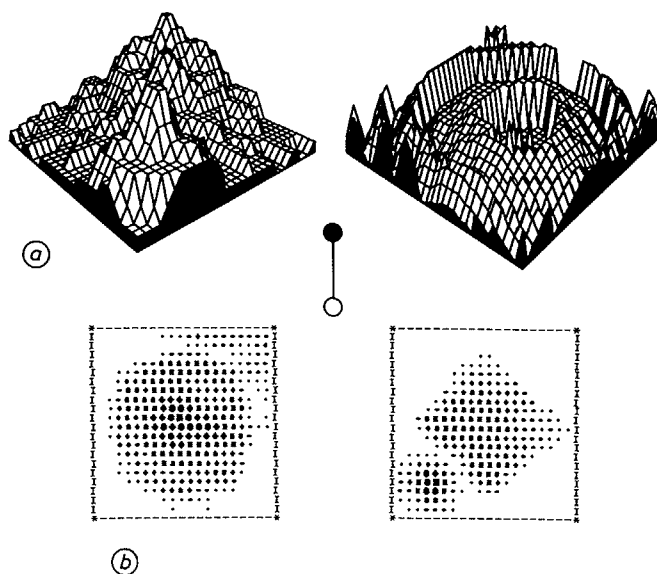hologram is only S/N=1/5.

Fig.7   Influence of hologram quantization on image re-
        construction.Object arrangement according to
        Fig. 4a

        a magnitude and phase of the complex hologram
          function
          magnitude: 10 quantization steps
          phase: 8 quantization steps
        b image reconstruction from a (objects 1 and 2)

ⓒ

ⓓ

c like a, but
   magnitude: 5 quantization steps
   phase: 4 quantization steps
d image reconstruction from c
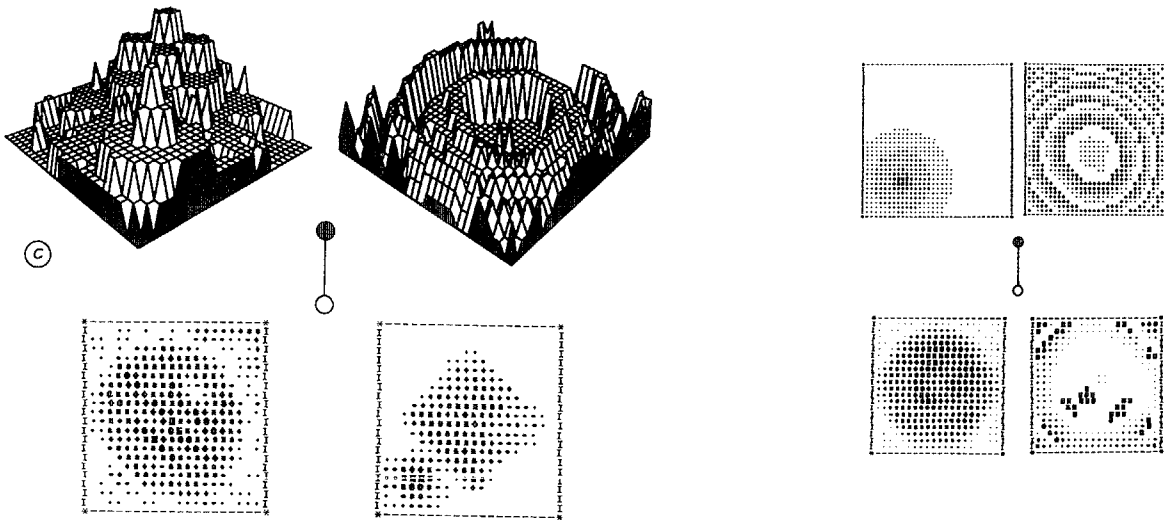

Fig.8   Influence of hologram quantization on image re-
        construction. Object 1 alone,magnitude and phase
        of the complex hologram function
        (magnitude: 5 quantization steps
         phase: 4 quantization steps)
        and the corresponding image reconstruction

5. RANGE DETERMINATION

As has already been reported in reference[6], the sum of
the magnitudes of the complex reconstructed object func-
tion $\underline{B}_{mn}$ in equation (2) over $m=0...M-1$ and $n=0...N-1$
yields an optimum if the variable distance z_p to the
hologram plane is equal to the real distance z_{real} of the
measuring plane. This is used to define an error function
for numerical range determination, which yields a mini-
mum for $z=z_{real}$.

$$EF_1(z_p) = \sum_{m=0}^{M-1}\sum_{n=0}^{N-1}\left\{1 - \left[\frac{B_{mn}(z_p)}{B_{mnMAX}(z_p)}\right]^\alpha\right\}^\beta \overset{!}{=} MIN \qquad (12)$$

It is advantageous to define a second criterion for range
determination, which uses the fact, that the reconstruc-
ted object shows its maximum picture sharpness if also
$z_p=z_{real}$. This leads to a second error function:

$$EF_2(z_p) = \left\{\sum_{m=0}^{M-1}\sum_{n=0}^{N-1}\frac{1}{\gamma}\left[|\Delta B(m)| + |\Delta B(n)|\right]\right\}^\rho \overset{!}{=} MIN \qquad (13)$$

where $\Delta B(m,n) = \frac{\partial B}{\partial x}dx + \frac{\partial B}{\partial y}dy$

$= \underbrace{[B(m,n) - B(m+1,n)]}_{\Delta B(m)} + \underbrace{[B(m,n) - B(m,n+1)]}_{\Delta B(n)}$
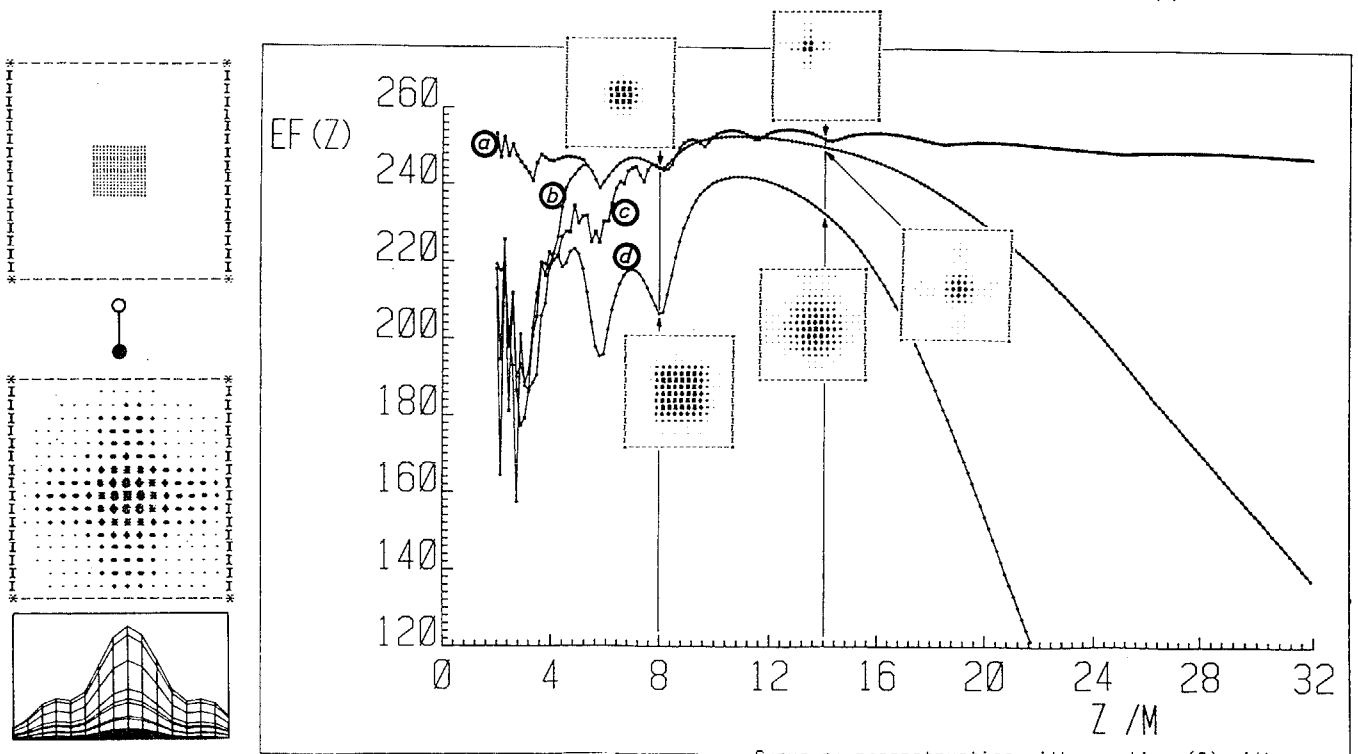

Fig.9   Range determination

        a with the amplitude density criterion, error
           function EF_1.
           Formation data: $x_M=y_N=2m$, length of side
           $a=0.5m, x_1=y_1=1m$, $x_{0I}=y_{0L}=1.92m$,
           $I=L=16$; $\lambda=0.03m$; $z_S=8m$, $x_{0S}=y_{0S}=1m$

Curve a: reconstruction with equation (2) with
          a window function; $x_M=y_N=2m,M=N=16$,
Curve b: like a, but without window function
Curve c: like a, but without window function
          and using the discrete Fourier trans-
          form algorithm
Curve d: like a, but without window function
          and $x_M=y_N=1m$, $x_n=y_n=0.5m$

Influence of Noise and Quantization Error in Microwave
Holography on Holograms and Image Reconstructions
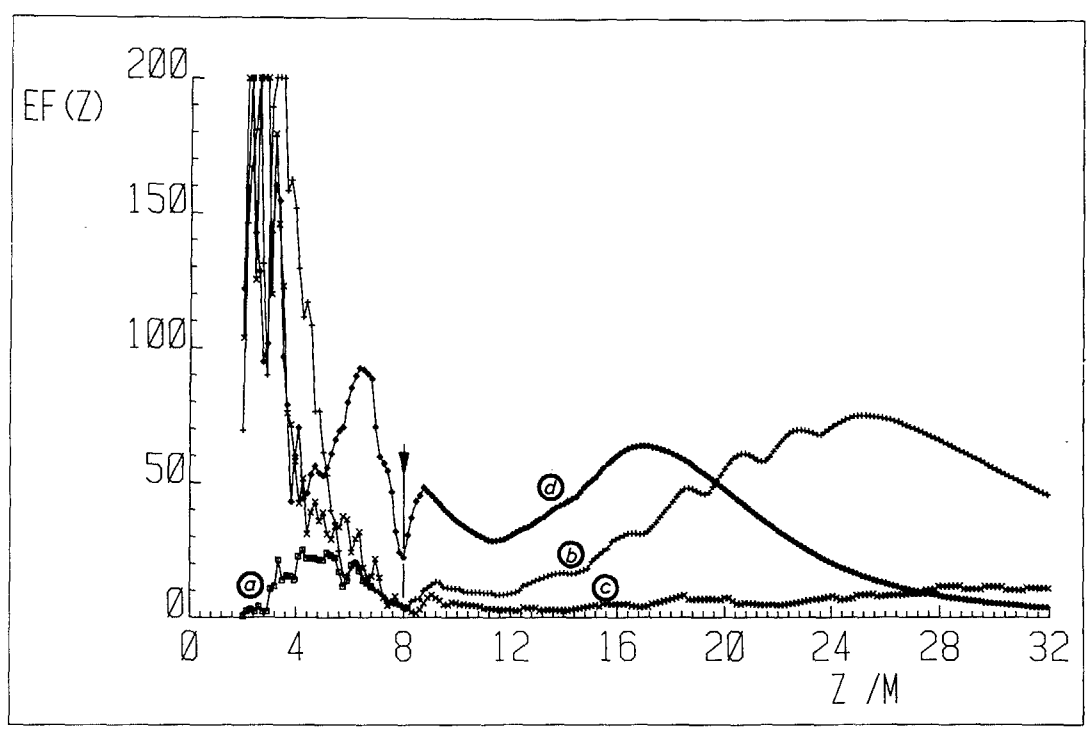
b corresponding curves for EF_2, $\gamma=4, \rho=2$.

In Fig. 9a error function EF_1 is investigated within a
longer distance range than in reference[6]. For a simple
object (quadratic plate) EF_1 is plotted versus distance
z for several numerical image reconstruction techniques.
Curve d is an error function appropriate for range
determination within a suitable z region of about 7 to
15m.

An investigation of the reconstruction techniques,
similar to those in Fig. 9a, for error function EF_2 (the
sharpness criterion) yields the result that a suitable
global minimum is accessible for range determination in
a wide distance range of about 2 to 22m (Fig. 9b). Fig.
10 shows the error function EF_2 versus distance for
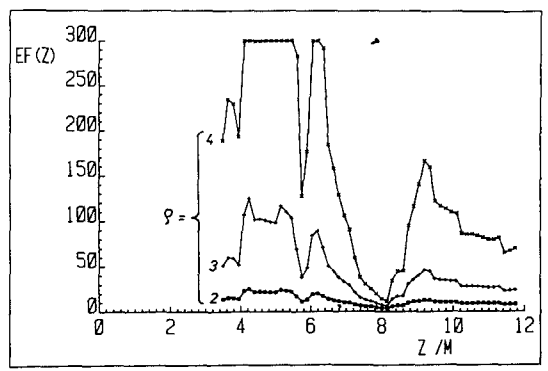several parameters ρ, cf. equation (13).

Fig.10 Range determination with the image sharpness
criterion, error function EF_2, cf. equation (13).
$\gamma=4, \Delta B_{min}=0.35$, $\lambda=0.03m$

The influence of the hologram bandwidth, which affects
the image sharpness, on the accuracy of the range
determination is demonstrated in Fig. 11. Triple band-
width (Fig.11b) increases the accuracy of error func-
ton EF_2 (the sharpness criterion) from +1.25% (Fig.11a)
to -0.4% (Fig.11b) while error function EF_1 (amplitude
density criterion) holds its accuracy within ±1.25%.
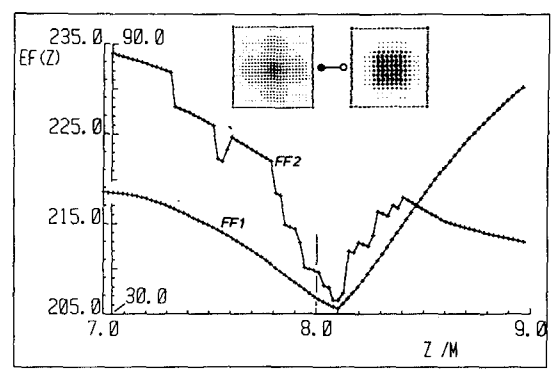
(a)
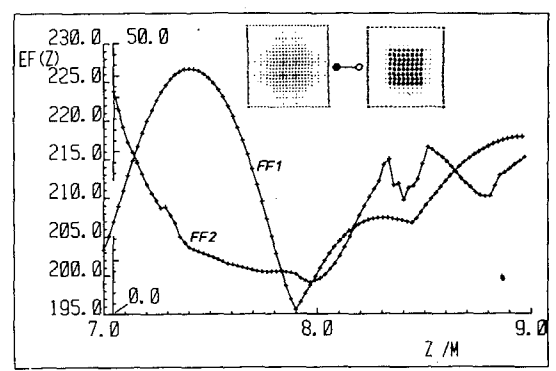
(b)

Fig.11 Influence of the hologram bandwidth on accuracy
of range determination
EF_1 amplitude density criterion
EF_2 sharpness criterion
$\alpha=3$, $\beta=2$, $\gamma=4$, $\rho=2$, $\Delta B_{min}=0.4$,

a $\lambda = 0.03m$
b $\lambda = 0.01m$ (triple bandwidth)

Fig. 12 shows that with the two error functions chosen a
range determination to within ±1.5% is possible even if
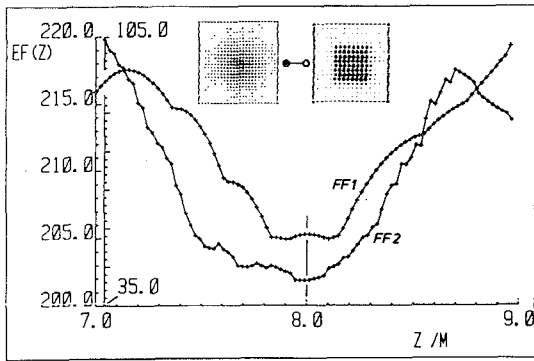the signal-to-noise ratio is S/N=2.

<u>Fig.12</u> Range determination at noisy signals. Signal-to-
noise ratio S/N=2
$\lambda = 0.015m$

For three-dimensional objects the real part of the com-
plex image reconstruction function can advantageously be
used to display separately distinct object parts. This
is demonstrated in Fig. 13, where a quadratic object
consisting of two plates of different sizes lo-
cated in different distances is investigated (Fig.13a).
Fig. 13b shows, that a clear separation of the distinct
object parts 1 and 2 is possible.

REFERENCES

1. F. Arndt, P. Ballerscheff, K.-H. Schierenbeck, and
    H. Ussat,
    "Hologrammsimulation und Bildrekonstruktion bei der
    Mikrowellenholographie". Arch.El.Übertragung, AEÜ-32,
    pp. 114-122,1978

2. A.P.Anderson,
    "Developments in microwave holography imaging".
    Proceedings of the 9th European Microwave Conference,
    Brighton, pp. 64-73, Sept. 1979

3. F. Arndt, and P. Ballerscheff,
    "Calculation and measurements of holograms and num-
    erical reconstruction of images in the microwave
    region". Proceedings, Septième Colloque sur le
    Traitement du Signal et ses Applications, Nice,pp.
    111/1-111/6, 1979

4. M.F.Adams, and A.P. Anderson,
    "Three dimensional image construction technique and
    its application to coherent microwave diagnostics".
    IEE Proc.-H, Microwave Optics and Antennas, Vol.127,
    pp.138-142, June 1980

5. G.Tricoles, E.L.Rope, and R.A. Hayward,
    "Improved design in microwave holographic images".
    IEEE Trans. Antennas and Propagation, vol. AP-29
    pp.320-326, March 1981

6. F. Arndt, and P. Ballerscheff,
    "Microwave holography for three-dimensional objects".
    Proceedings, Huitième Colloque sur le Traitement
    du Signal et ses Applications, Nice, pp. 809-814,
    1981

7. C.Rint,
    "Handbuch für Hochfrequenz- und Elektrotechniker".
    Band II, Hüthig und Pflaum Verlag, München/Heidelberg,
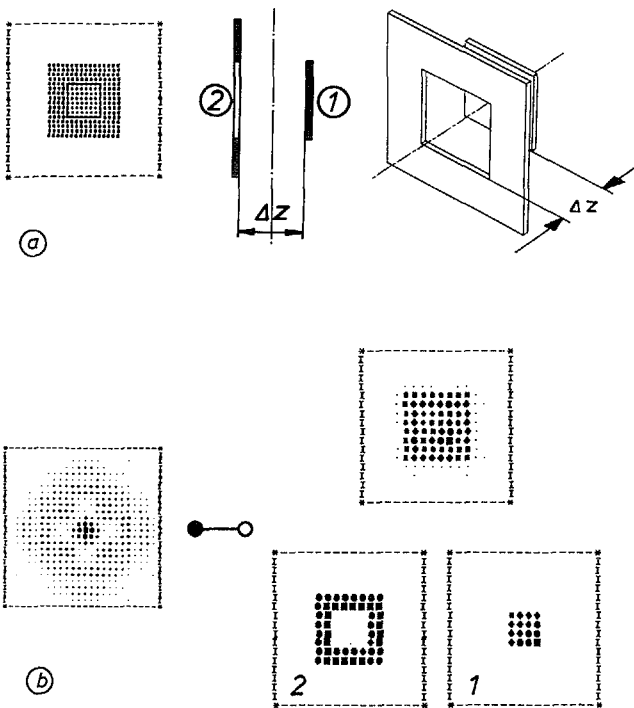   1978, 12. Auflage, S.157.

<u>Fig.13</u> Separation of distinct object parts in image re-
construction of three-dimensional objects

a quadratic plate behind the remaining frame at
a distance $\Delta z=(2n-1)\cdot\lambda/4$
b magnitude of hologram and image reconstruction
regarding the real parts
$\lambda=0.01m$